Molecular Pharmacology Fast Forward. Published on October 20, 2015 as DOI: 10.1124/mol.115.100693
This article has not been copyedited and formatted. The final version may differ from this version.

Molecular interactions and implications of aldose reductase inhibition by PGA_1 and clinically used prostaglandins

Beatriz Díez-Dacal, Francisco J. Sánchez-Gómez, Pedro A. Sánchez-Murcia, Ivana Milackova, Tahl Zimmerman, Jana Ballekova, Elena García-Martín, José A. G. Agúndez, Severine Gharbi, Federico Gago, Milan Stefek, Dolores Pérez-Sala

Chemical and Physical Biology Department, Centro de Investigaciones Biológicas, Consejo Superior de Investigaciones Científicas (C.S.I.C.), Madrid, Spain (B.D.-D., F.J.S.-G., T.Z., D.P.-S.); Department of Biomedical Sciences, Universidad de Alcalá, E-28871 Alcalá de Henares, Madrid, Spain (P.S.-M., F.G.); Institute of Experimental Pharmacology and Toxicology. Slovak academy of sciences, SK-841 04 Bratislava, Slovakia (I.M., J.B., M.S.); Department of Pharmacology, University of Extremadura, Spain (E.G.-M., J.A.G.A.); Centro Nacional de Biotecnología (C.S.I.C.), Madrid, Spain (S.G.)

Molecular Pharmacology Fast Forward. Published on October 20, 2015 as DOI: 10.1124/mol.115.100693
This article has not been copyedited and formatted. The final version may differ from this version.

Running title: Prostaglandins inhibit aldose reductase

Please address correspondence to:

Dr. Dolores Pérez-Sala

Department of Chemical and Physical Biology

Centro de Investigaciones Biológicas, C.S.I.C.

Ramiro de Maeztu, 9, 28040 Madrid, Spain

Phone: 34918373112

FAX: 34915360432

Email: dperezsala@cib.csic.es

No. of text pages: 34

No. of tables: 0

No. of figures: 9

No of references: 60

No. of words in the abstract: 239

No. of words in the introduction: 471

No. of words in the discussion: 1394

Abbreviations: AKR, aldo-keto reductase; cyPG, cyclopentenone prostaglandin; GSH, glutathione; GSNO, nitrosoglutathione; GST, glutathione transferase; PG, prostaglandin.

Molecular Pharmacology Fast Forward. Published on October 20, 2015 as DOI: 10.1124/mol.115.100693
This article has not been copyedited and formatted. The final version may differ from this version.

Abstract

Aldose reductase (AKR1B1) is a critical drug target due to its involvement in diabetic complications, inflammation and tumorigenesis. However, to date, development of clinically useful inhibitors has been largely unsuccessful. Cyclopentenone prostaglandins (cyPGs) are reactive lipid mediators that bind covalently to proteins and exert anti-inflammatory and antiproliferative effects in numerous settings. By pursuing the targets for modification by cyPGs we have found that the cyPG PGA_1 binds to and inactivates AKR1B1. A PGA_1-AKR1B1 adduct was observed, both by MALDI-TOF MS and by SDS-PAGE using biotinylated PGA_1 (PGA_1-B). Insight into the molecular interactions between AKR1B1 and PGA_1 was advanced by molecular modeling. This anticipated the addition of PGA_1 to active site Cys298 and the potential reversibility of the adduct, which was supported experimentally. Indeed, loss of biotin label from the AKR1B1-PGA_1-B adduct was favored by glutathione, indicating a retro-Michael reaction, which unveils new implications of cyPG-protein interaction. PGA_1 elicited only marginal inhibition of aldehyde reductase (AKR1A1), considered responsible for the severe adverse effects of many AKR1B1 inhibitors. Interestingly, other PGs, including non-electrophilic PGE_1 and PGE_2, currently used in the clinical practice, inhibited the enzyme. Moreover, both PGA_1 and PGE_1 reduced the formation of sorbitol in an ex-vivo model of diabetic cataract to extents comparable to those attained by the known AKR inhibitor epalrestat. Taken together, these results highlight the role of PGs as AKR1B1 inhibitors and the interest of PG-related molecules as leads for the development of novel pharmacological tools.

Molecular Pharmacology Fast Forward. Published on October 20, 2015 as DOI: 10.1124/mol.115.100693
This article has not been copyedited and formatted. The final version may differ from this version.

Introduction

Enzymes of the Aldo-Keto Reductase (AKR) family metabolize various aldehydes using NAD(P)(H) as a cofactor. Although they play a protective role under physiological situations, their increased activity is considered a pathogenic factor (Alexiou et al., 2009). Aldose reductase (AKR1B1) is an important mediator of inflammation and diabetic complications (Alexiou et al., 2009; Laffin and Petrash, 2012; Srivastava et al., 2011). AKR1B1 metabolizes reactive aldehydes, like 4-hydroxy-trans-2-nonenal (Ramana et al., 2006) yielding products that perpetuate inflammation (Srivastava et al., 2011). AKR1B1 has also been involved in allergic inflammation and asthma (Yadav et al., 2013; Yadav et al., 2011). Moreover, AKR1B1 participates in the metabolism of certain prostaglandins (PGs), thus regulating the generation of inflammatory or vasoactive mediators (Kabututu et al., 2009; Michaud et al., 2014).

AKR1B1 metabolizes glucose through the polyol pathway producing sorbitol. In hyperglycemia this provokes sorbitol accumulation, inducing osmotic stress, favoring epithelial-mesenchymal transition (Ko et al., 1997; Zhang et al., 2012), and contributing to fibrosis, diabetic cataract, and vasculopathy (Hashim and Zarina, 2012; Lai et al., 2013). In addition, increased AKR1B1 activity depletes NADPH required for cellular antioxidant defenses and detoxifying systems (Pollak et al., 2007b), thus increasing susceptibility to oxidative stress (Pollak et al., 2007a; Ying, 2008). Moreover, AKR1B1 can elicit a proinflammatory and prothrombotic state in diabetes through oxidative stress (Tang et al., 2011) or Egr-1 hyperacetylation and activation (Vedantham et al., 2014).

Consequently, the search for AKR1B1 inhibitors is an active field of research. However, the clinical use of various compounds, including tolrestat (Drugbank ID DB02383) and sorbinil (Drugbank ID DB02712) has been hampered by their poor effectiveness and severe adverse effects, such as hepatitis or renal toxicity, attributed to inhibition of the related enzyme aldehyde reductase (AKR1A1 or ALR1) (Muthenna et al., 2009). Therefore, inhibitor selectivity for AKR1B1 over AKR1A1 is preferred over inhibitory potency if it implies less side effects (Suzen and Buyukbingol, 2003).

Molecular Pharmacology Fast Forward. Published on October 20, 2015 as DOI: 10.1124/mol.115.100693
This article has not been copyedited and formatted. The final version may differ from this version.

cyPGs are electrophilic compounds that form Michael adducts with proteins, mainly at cysteine residues located in favorable environments (Garzón et al., 2011; Oeste and Pérez-Sala, 2014). cyPGs bind to and modulate transcription factors (Cernuda-Morollón et al., 2001; Kim and Surh, 2006; Pérez-Sala, 2011), activate the antioxidant response (Levonen et al., 2004; Martínez et al., 2012), inactivate detoxifying enzymes, like glutathione transferases (Sánchez-Gómez et al., 2010), and induce anti-inflammatory and antiproliferative effects (Díez-Dacal and Pérez-Sala, 2012), for which they have been proposed as therapeutic tools (Fukushima et al., 2001; Homem de Bittencourt et al., 2007).

Recently, we identified several AKRs as potential targets for the cyPG PGA_1 (Díez-Dacal et al., 2011). Here we have explored the interaction of PGA_1 with AKR1B1. Our results show that PGA_1 inactivates AKR1B1 by interacting at its active site, and reduces sorbitol formation in an ex-vivo model of diabetic cataract. Remarkably, clinically-available PGs bind to and inhibit AKR1B1, opening novel perspectives for the development of inhibitors.

Molecular Pharmacology Fast Forward. Published on October 20, 2015 as DOI: 10.1124/mol.115.100693
This article has not been copyedited and formatted. The final version may differ from this version.

Materials and Methods

Materials. Prostaglandins (PGs) and PG analogs were from Cayman Europe. Recombinant AKR1B1 from various sources was used in this study (Wako Chemicals USA, Inc. Richmond, VA; Prospec-Tany TechnoGene Ltd., Ness Ziona, Israel; Acris Antibodies GmbH, Herford, Germany). In addition, some assays were performed with aldose reductase purified from rat lens (AKR1B4) (see below). Recombinant human aldehyde reductase (AKR1A1) was from MyBiosource. In some assays, aldehyde reductase purified from rat kidney (AKR1A3) was used. Essentially the same results were obtained with enzymes from different sources. Anti-aldose reductase antibody (anti-AKR, sc-33219) and anti-AKR1A1 (sc-365078) were from Santa Cruz Biotechnology, specific anti-AKR1B1 was from Abcam. Other reagents were from Sigma. The peptide ^{297}VCALLSCTSHK^{307} from the sequence of human AKR1B1 was synthesized at the Protein Chemistry facility of C.I.B.

Interaction of prostaglandins with AKR1B1 in vitro. Prostaglandins were dissolved in DMSO. AKR1B1 at 5 μM was incubated in 20 mM Tris-HCl pH 7.0, 45 mM NaCl, 5 mM $MgCl_2$, 0.1 mM DTT, in the presence of PGs at the indicated concentrations or vehicle for 2 h at r.t., after which, incubation mixtures were directly used for MS analysis or denatured by addition of 1% TFA and 5 M guanidinium chloride, final concentrations, before purification on ZipTip C4 (Millipore), from which protein was eluted with 75% acetonitrile. Interaction of AKR1B1 with biotinylated PGs was assessed by incubation under the same conditions as above, after which, incubation mixtures were analyzed on 10% SDS-polyacrylamide gels. Gels were transferred to Immobilon P membranes and the biotin signal associated with the protein was visualized by incubation with HRP-streptavidin and ECL detection. For analysis of the interaction between PGA_1 and the AKR1B1 ^{298}VCALLSCTSHK^{307} peptide, a 100 μM solution of the peptide in water was incubated with 500 μM PGA_1 in the presence of 0.5 mM DTT at r.t. for 16 h. The integrity of the PG under the incubation conditions used was routinely checked by LC-MS at the Protein Chemistry facility of C.I.B.

Molecular Pharmacology Fast Forward. Published on October 20, 2015 as DOI: 10.1124/mol.115.100693
This article has not been copyedited and formatted. The final version may differ from this version.

MS analysis. For analysis of full-length AKR1B1, 2 µl of the incubation mixtures were mixed with 2 µl of 2% TFA and 2 µl of a suspension of the matrix (2,5-dihydroxy-acetophenone, Bruker-Daltonics). One µl of this mixture was applied to the sample plate (MTP384 800 µm AnchorChip, Bruker Daltonics) for crystallization at r.t. before analysis on an Autoflex III MALDI-TOF-TOF mass spectrometer (Bruker Daltonics) equipped with a Smartbeam laser, operating in the linear mode. Analysis of the purified peptide was carried out by MALDI-TOF MS. Peptide fragmentation was achieved by MALDI-TOF-TOF MS-MS for sequence analysis and determination of the modification site. One µl of peptide was mixed with 1 µl of the matrix (α-ciano-4-hydroxycinnamic acid (Bruker-Daltonics) at 3 mg/ml in 33% acetronitrile (v/v) and 0.1% (v/v) trifluoroacetic acid. One µl of this mixture was applied to the sample plate. MALDI-MS and MALDI-MS/MS data were obtained manually in an Autoflex III MALDI-TOF-TOF mass spectrometer equipped with a LIFT-MS/MS device. Data analysis was performed with the FlexAnalysis software (Bruker-Daltonics). Analyses were carried out at the Proteomics and Genomics facility of C.I.B.

Animals. Male Wistar rats 8 - 9 weeks old, weighing 200 - 230 g, were used as organ donors. The animals came from the Breeding Facility of the Institute of Experimental Pharmacology Dobra Voda (Slovak Republic). The study was approved by the Ethics Committee of the Institute and performed in accordance with the Principles of Laboratory Animal Care (NIH publication 83-25, revised 1985) and the Slovak law regulating animal experiments (Decree 289, Part 139, July 9th 2003).

Preparation of aldose reductase (ALR2 or AKR1B4) from rat lens. AKR1B4 from rat lens was partially purified using a procedure as follows: lenses were quickly removed from rats following euthanasia and homogenized in a glass homogenizer with a teflon pestle in 5 volumes of cold distilled water. The homogenate was centrifuged at 10,000 x g at 0-4°C for 20 min. The supernatant was precipitated with saturated ammonium sulfate at 40 %, 50 % and then at 75 % salt saturation. The supernatant was retained after the first two precipitations. The pellet from the last step, possessing AKR1B4 activity, was

Molecular Pharmacology Fast Forward. Published on October 20, 2015 as DOI: 10.1124/mol.115.100693
This article has not been copyedited and formatted. The final version may differ from this version.

dispersed in 75 % ammonium sulfate and stored in smaller aliquots in liquid nitrogen container.

Preparation of aldehyde reductase (ALR1 or AKR1A3) from rat kidney. AKR1A3 from rat kidney was partially purified as follows: kidneys were quickly removed from rats following euthanasia and homogenized in a knife homogenizer followed by processing in a glass homogenizer with a teflon pestle in 3 volumes of 10 mM sodium phosphate buffer, pH 7.2, containing 0.25 M sucrose, 2.0 mM EDTA dipotassium salt and 2.5 mM β-mercaptoethanol. The homogenate was centrifuged at 16 000 x g at 4°C for 30 min and the supernatant was subjected to ammonium sulfate fractional precipitation at 40 %, 50 % and 75 % salt saturation. The pellet obtained from the last step, possessing AKR1A3 activity, was dissolved in 10 mM sodium phosphate buffer, pH 7.2, containing 2 mM EDTA dipotassium salt and 2 mM β-mercaptoethanol to achieve total protein concentration of approximately 20 mg/ml. DEAE DE 52 resin was added to the solution (33 mg/ml) and after gentle mixing for 15 min removed by centrifugation. The supernatant containing AKR1A3 was then stored in small aliquots in liquid nitrogen. No appreciable contamination by AKR1B4 in AKR1A3 preparations was detected since no activity in terms of NADPH consumption was observed in the presence of glucose substrate up to 150 mM.

Enzyme activity assays. Assays were performed according to slightly different protocols depending on the source of enzyme, recombinant proteins or partially purified preparations. For assay of recombinant AKR1B1 activity, 2 μg of protein was incubated with 10 mM D,L-glyceraldehyde and 200 μM NADPH in 100 mM sodium phosphate buffer, pH 6.8 in a total volume of 850 μl in a spectrometer cuvette. Assay was started by the addition of protein and was carried out for 5 min at 24ºC. Enzymatic activity was monitored as the consumption of NADPH measured by the decrease in the absorbance at 340 nm (ε 340nm, NADPH = 6200 M^{-1} cm^{-1}), in an Ultrospec 4300-pro spectrophotometer (Amersham Biosciences). Where indicated, the recombinant protein was preincubated with PGA_1 before the assay. Recombinant AKR1A1 activity was assayed in 100 mM potassium phosphate buffer, pH 7.2 using 100 μM NADPH and 45 mM D-glucuronate. Assay was

Molecular Pharmacology Fast Forward. Published on October 20, 2015 as DOI: 10.1124/mol.115.100693
This article has not been copyedited and formatted. The final version may differ from this version.

started by addition of the protein and incubations were carried out at room temperature for 4 min. Consumption of NADPH was assessed as above. Spontaneous decrease of NADPH was routinely monitored using assay mixtures without enzyme. All assays were performed at least three times in duplicates. PGs were added to the incubation prior or at the time of the assay, as indicated, in DMSO. Final concentration of DMSO in assays was 1%. Control samples were incubated in the presence of an equivalent volume of DMSO.

For assay of AKR1B4 and AKR1A3 partially purified preparations from rat tissues the following procedures were followed: To determine AKR1B4 activity, the reaction mixture contained 4.67 mM D,L-glyceraldehyde as a substrate, 110 μM NADPH, 67 mM phosphate buffer, pH 6.2 and 50 μl of the enzyme preparation in a total volume of 1.5 ml. The reference blank contained all the above reagents except the substrate D,L-glyceraldehyde to correct for oxidation of NADPH not associated with reduction of the substrate. The enzyme reaction was initiated by addition of D,L-glyceraldehyde and was monitored for 4 min after an initial period of 1 min at 30 °C. AKR1A3 activity was assayed using 20 mM D-glucuronate as a substrate in the presence of 120 μM NADPH in 100 mM phosphate buffer pH 7.2 at 37°C. Enzyme activities were monitored as NADPH consumption by the decrease of absorbance at 340 nm and were expressed as (O.D.)/s/mg protein. Enzyme activities were adjusted by diluting the enzyme preparations with distilled water so that 50 μl of the enzyme preparation gave an average reaction rate for the control sample of 0.020 ± 0.005 absorbance units/min. The effect of PGA_1 on the enzyme activity was determined by adding PGA_1 at the required concentrations dissolved in DMSO (1% final concentration of DMSO in incubation mixture), immediately or 1 hour before activity measurement. The inhibitor at the same concentration was included in the reference blank. Control samples received an equivalent amount of DMSO. The preincubation was performed in the absence of NADPH. At the end of the preincubation period NADPH was added at the required concentration and the enzyme reaction was started by addition of an appropriate amount of substrate (D,L-glyceraldehyde or D-glucuronate).

Molecular Pharmacology Fast Forward. Published on October 20, 2015 as DOI: 10.1124/mol.115.100693
This article has not been copyedited and formatted. The final version may differ from this version.

IC50 values were calculated from a sigmoidal dose-response curve obtained with the GraphPad Prism software.

Determination of sorbitol formation by isolated rat lenses. A previously described protocol was used (Chatzopoulou et al., 2011), with the exception that Sigma M-199 (M 3769) was used as an incubation medium at pH 7.4. Briefly, freshly dissected lenses were incubated individually in 1.5 ml of M-199 medium for 3 h at 37ºC, into which 5% CO_2, 95% O_2 was bubbled at regular intervals. PGA_1 prepared in DMSO was added to incubation mixtures in such a way that the final DMSO concentration in all incubations was 1%. Incubations were terminated by placing the mixtures on ice, washing the eye lenses with PBS and freezing them at -80ºC until analysis. For sorbitol measurement, thawed eye lenses were homogenized in distilled water and subjected to precipitation with ice-cold $HClO_4$, centrifugation and neutralization of the supernatant with K_2CO_3. Sorbitol present in the supernatant was determined enzymatically by a previously published method, based on its oxidation to fructose by sorbitol dehydrogenase coupled to the reduction of resazurin by diaphorase to the highly fluorescent resorufin (Mylari et al., 2003).

Molecular modeling. The Cartesian coordinates of AKR1B1 were taken from the 1.65 Å resolution crystal structure of $NADP^+$-bound human aldose reductase (PDB entry: 1ADS). Protonation of titratable groups and assignment of AMBER leaprc.ff14SB force-field parameters was performed as described previously (Díez-Dacal et al., 2011). Atom charges for free and Cys298-bound PGA_1 atoms were obtained by fitting the quantum mechanically calculated (RHF 6-31G*\\3-21G*) molecular electrostatic potential to a point charge model, as implemented in Gaussian 03 (Gaussian, Inc.) using the R.E.D. server (URL: http://q4md-forcefieldtools.org/REDServer/). Parameters for both NADP(H) cofactors were taken from the AMBER parameter database from the Bryce Group of the University of Manchester (URL: http://www.pharmacy.manchester.ac.uk/bryce/amber/).

The noncovalent and covalent AKR1B1:NADP(H):PGA_1 and AKR1B1:$NADP^+$:PGA_1 ternary complexes were modeled as described before (Díez-Dacal et al., 2011) and immersed in octahedra containing explicit TIP3P water molecules and 4 Na^+ ions to

Molecular Pharmacology Fast Forward. Published on October 20, 2015 as DOI: 10.1124/mol.115.100693
This article has not been copyedited and formatted. The final version may differ from this version.

achieve electroneutrality. Unrestrained molecular dynamics simulations were run for 20 ns using the AMBER force field under periodic boundary conditions and program *pmemd* as implemented in the AMBER14 suite (Case et al., 2015). Program Glide (Schrödinger, SL) was used for docking glutathione (GSH) and the final binding mode was refined after selecting 3 conformations of covalently bonded PGA_1.

Statistical analysis. All assays were repeated at least three times. Statistical significance was evaluated by a parametric Student´s *t*-test for independent samples.

Molecular Pharmacology Fast Forward. Published on October 20, 2015 as DOI: 10.1124/mol.115.100693
This article has not been copyedited and formatted. The final version may differ from this version.

Results

PGA_1 inactivates AKR1B1. Incubation of recombinant AKR1B1 with PGA_1 inhibited enzyme activity in a concentration-dependent manner (Fig. 1A). An IC50 of 15.9 ± 7.4 μM (average of 4 assays ± SEM) was obtained. Inhibition of AKR1B1 by PGA_1 was also time-dependent. AKR1B1 was incubated with PGA_1 (20 μM) for increasing times and the pre-incubation mixture was diluted 1:10 prior to enzyme assay. Under these conditions, close to 40% inhibition of the enzymatic activity was observed after a 2 h pre-incubation with PGA_1 (Fig. 1B), indicating an inactivation of the enzyme. To provide further evidence for this effect, AKR1B1 was incubated with increasing concentrations of PGA_1 for 2 h, after which, enzyme activity was assayed maintaining the concentration of PG in the assay mixture or diluting it 10 times (Fig. 1C). Consistent with the previous results, dilution of the PG in the assay partially improved but did not completely restore enzyme activity (Fig. 1C). Thus, for any given concentration of the PG in the assay the degree of inhibition observed was always higher when the enzyme had been pre-incubated with a 10-fold PG excess. These results indicate that PGA_1 inactivates AKR1B1.

PGA_1 binds covalently to AKR1B1. To assess the possibility of a covalent interaction between PGA_1 and AKR1B1, we first analyzed PGA_1-binding to AKR1B1 by MALDI-TOF MS (Fig. 2A). The intact control protein was observed at *m/z* 35686.1. In the presence of PGA_1 we observed a mass shift of 336.9, compatible with the formation of a complex between one PGA_1 molecule (mass 336.5 Da) and AKR1B1. PGA_1 binding was stable even after incubation in the presence of 5 M guanidinium chloride and subsequent purification by ZipTip (Fig. 2A, lower panel). In addition, incubation of AKR1B1 with the biotinylated analog of PGA_1 (PGA_1-B) resulted in the formation of a complex that could be detected under denaturing conditions, as assessed by SDS-PAGE followed by protein transfer and biotin detection with HRP-coupled streptavidin (Fig. 2B). These results firmly support the covalent nature of the PGA_1-AKR1B1 complex.

Molecular modeling of PGA_1-AKR1B1 interaction. In our previous study we proposed a three-dimensional molecular model for the pre-covalent complex between PGA_1 and

Molecular Pharmacology Fast Forward. Published on October 20, 2015 as DOI: 10.1124/mol.115.100693
This article has not been copyedited and formatted. The final version may differ from this version.

AKR1B1 (Díez-Dacal et al., 2011). We suggested that PGA_1 was likely to share some binding features with several known inhibitors which have been co-crystallized with AKR1B1, the most prominent being that the cyclopentenone oxygen (O9) of PGA_1, in analogy to the carboxylate of many of these inhibitors, can accept hydrogen bonds from both the Nε of His111 and the hydroxyl of Tyr49 (Fig. 3). In such an arrangement, the β-carbon of the α,β-unsaturated system in PGA_1 (C11) is activated and able to react with the attacking sulfur of Cys298 to yield the corresponding Michael adduct (Fig. 3A). The reaction mechanism would first proceed with the formation of an enolate intermediate which would then evolve to the keto form following protonation at C10. Although addition of cyPGs to cysteine residues is considered virtually irreversible in biological systems, theoretically, this reaction can proceed in both ways. In fact, in the case of GSTp, excess glutathione (GSH) has been proposed to facilitate the retro-Michael reaction of a GSTp-PGA_2 adduct (van Iersel et al., 1999). Therefore, we assessed the feasibility of GSH binding to the AKR1B1(Cys298-PGA_1):$NADP^+$ ternary complex using molecular modeling. Our results showed that the attacking sulfur group in GSH can indeed gain access to C11 of PGA_1 and therefore, this metabolite could reverse the covalent binding of PGA_1 to the enzyme through a Michael addition (Fig. 3B). Remarkably, the reversibility could be confirmed experimentally by incubating the AKR1B1-PGA_1-B adduct in the presence of excess GSH. This induced a loss of the biotin signal associated with AKR1B1 that is indicative of a decrease in the concentrations of adduct (Fig. 4A). Complementarily, an excess nitro-benzyl-glutathione analog (NBG), in which the thiol group of glutathione is blocked, did not show this effect (Fig. 4B). It is noteworthy that when the PGA_1-B adduct of the AKR1B10 isoform was likewise incubated with GSH, the biotin signal was also reduced (Fig. 4C). These results suggest that the covalent PGA_1-AKR1B1 adduct may be reversible under certain conditions and that this behavior may be shared by other members of the AKR family, given the high degree of conservation of the catalytic residues.

Next, we attempted to confirm the binding site of PGA_1 to AKR1B1 using several strategies. The first one relied on direct MS analysis of modified recombinant AKR1B1 using both MALDI/MS and LC-MS/MS approaches. AKR1B1 was incubated with PGA_1 and protein

Molecular Pharmacology Fast Forward. Published on October 20, 2015 as DOI: 10.1124/mol.115.100693
This article has not been copyedited and formatted. The final version may differ from this version.

was digested with trypsin under various conditions, including protein reduction and/or alkylation. When cysteines were reduced and alkylated prior to trypsin digestion, all the cysteine-containing peptides were identified and displayed carbamidomethylation modification. In the condition without reduction and alkylation we reached maximal protein coverage of 92%, but we did not detect modified peptides in the PGA_1-incubated protein. However, the peptide containing Cys298 was not identified under this condition, suggesting that it could be particularly unfavorable for detection using this technique due to poor ionization or to the occurrence of uncharacterized modifications. Additionally, processing of the sample for analysis could affect the stability of the PGA_1 adduct. To get insight into these possibilities we next tested the direct interaction of the synthetic tryptic peptide that corresponds to the C-terminal region, ^{297}VCALLSCTSHK^{307} (*m/z* 1161.5), with PGA_1 under forced conditions. Indeed, we observed the modification of the peptide by PGA_1 addition, resulting in a mass shift of 336.5 Da (*m/z* of the modified peptide 1498.1; expected *m/z* of the modified peptide 1498.2), which corresponds to the incorporation of one PGA_1 molecule (Fig. 5). MALDI-TOF-TOF MS/MS analysis of the modified peptide revealed binding of PGA_1 at Cys298, as indicated by the detection of peaks compatible with a mass increment of 336.5 on several ions (see details in Figure 5A). In addition, we observed several peaks compatible with PGA_1 addition at Cys303, suggesting that the 1498.1 peptide may contain a mixture of both species. Moreover, the ion corresponding to the retro-Michael fragmentation of the modified peptide (*m/z* 1161.5) as well as the ions corresponding to the free cysteines, were detected. Thus, although using this approach we can observe modification of cysteine residues by PGA_1, binding is not fully stable under the conditions of the analysis and does not allow to ascertain the potential selectivity of the modification. Moreover, the isolated peptide cannot mimic the complex interactions taking place in the full-length protein. Therefore, to strengthen the hypothesis that PGA_1 binds at the active site Cys298 we performed a competition assay with GSNO, which has been shown to specifically target Cys298 by inducing its glutathionylation (Baba et al., 2009). As observed in Fig. 5B, preincubation of AKR1B1 with GSNO reduced the incorporation of PGA_1-B, thus suggesting that Cys298 glutathionylation impairs the formation of the adduct.

Molecular Pharmacology Fast Forward. Published on October 20, 2015 as DOI: 10.1124/mol.115.100693
This article has not been copyedited and formatted. The final version may differ from this version.

Various PGs inhibit AKR1B1 activity. Recent works have documented the interaction of several PGs with enzymes of the AKR family (Nagata et al., 2011), and the role of AKR1B1 in PG synthesis (Kabututu et al., 2009). Therefore, we explored the effect of several PGs as potential inhibitors of AKR1B1. The structures of the various compounds used are depicted in Figure 6A. Both 15d-PGJ_2 and its analog lacking the endocyclic double bond, 9,10-dihydro-15d-PGJ_2, inhibited AKR1B1 activity in vitro with IC50 values of 17.0 and 27.3 μM, respectively. Both compounds are capable of forming covalent adducts with proteins. Interestingly, several non-electrophilic PGs, including PGE_2 and PGE_1, the precursor of PGA_1, as well as the PGE_1 analog limaprost (17α,20-dimethyl-Δ^2-PGE_1), could also inhibit AKR1B1 (IC50 values of several of the assayed compounds are depicted in Figure 6B). This is important because PGE_1 and its analogs are currently used in the clinical practice as vasodilators in multiple situations, including erectile dysfunction, patent ductus arteriosus or intermittent claudication (Hanchanale and Eardley, 2014; Nakanishi et al., 2008; Swainston Harrison and Plosker, 2007; Talosi et al., 2004). To get insight into the nature of the interaction between PGE_2 and AKR1B1, we performed MALDI-TOF MS analysis (Fig. 7A). AKR1B1 incubated in the presence of PGE_2 showed a displacement of the centroid of the protein by 349.6 Da, which is compatible with the formation of a PGE_2-AKR1B1 complex (mass of PGE_2, 352.5)(Fig. 7A, upper panel). This complex was stable after addition of 1.5 M guanidinium chloride and ZipTip purification. However, in contrast to what was observed with PGA_1, binding of PGE_2 was lost after addition of 5 M guanidinium chloride and subsequent purification on ZipTip (Fig. 7A, lower panel). Furthermore, incubation of AKR1B1 with biotinylated PGE_2 did not result in an adduct stable under SDS-PAGE denaturing conditions (Fig. 7B). Thus, these observations suggest that PGE also interacts with the enzyme active site, although through a non-covalent interaction. Consistent with this, incubation of AKR1B1 with an excess PGA_1 or PGE_2 reduced its modification by PGA_1-B (Fig. 7C, left panels). However, when the excess of competing PG was removed prior to addition of PGA_1-B the blocking effect of PGE_2 was abolished whereas that of PGA_1 persisted (Fig. 7C, right panels). These results indicate that some PGs may tightly bind to AKR1B1 in such a way that the complex is stable under the

Molecular Pharmacology Fast Forward. Published on October 20, 2015 as DOI: 10.1124/mol.115.100693
This article has not been copyedited and formatted. The final version may differ from this version.

conditions used for MALDI-TOF MS but is lost under denaturing conditions or upon removal of the PG. Therefore, several PGs can act as inhibitors of AKR1B1, at least in part by interacting with the protein in either a reversible or an irreversible manner.

PGA_1 selectively inhibits AKR1B1 versus AKR1A1. An important issue about AKR1B1 inhibitors is their selectivity towards this enzyme versus other enzymes processing aldehydes, mainly aldehyde reductase or AKR1A1, since inhibition of AKR1A1 has been considered responsible for some of the adverse effects of aldose reductase inhibitors (Alexiou et al., 2009). Therefore, we assessed whether PGA_1 inhibited AKR1A1. PGA_1 inhibited recombinant AKR1A1 only marginally (200 μM PGA_1 elicited an inhibition of AKR1A1 close to 20%, Fig. 8). Moreover, the inhibition was not concentration-dependent, which precluded the calculation of an IC50 value. Similar results were obtained using enzymes from different sources, namely, the recombinant enzyme and the enzyme purified from rat kidney. In the case of rat kidney aldehyde reductase, the percentage inhibition by 100 μM PGA_1 was 18.8% ± 3.1 (average ± SD of 6 determinations) without preincubation, and 17.8% ± 1.2 (average ± SD of 3 determinations), after 1 h preincubation. Therefore, preincubation with PGA_1 did not influence the extent of inhibition. Thus, PGA_1 displays high selectivity for AKR1B1 versus AKR1A1.

Studies with aldose reductase (AKR1B4) from rat lens. To obtain insight into the potential beneficial effects of inhibiting AKR1B1 in a biological system, we studied rat lenses as a model in which AKR1B4 activity has been involved in the development of diabetic cataract (Reddy et al., 2011). PGA_1 effectively inhibited AKR1B4 isolated from rat lens with an IC50 of 4.1 ± 1.1 μM. Also in this case, preincubation of the enzyme preparation with the PG inactivated the enzyme, as deduced from the stronger inhibition observed: percentage of inhibition observed with 5 μM PGA_1, 52.46 ± 1 (average ± SEM of nine assays); percentage of inhibition after 1 h preincubation in the presence of 5 μM PGA_1, 66.10 ± 0.53 (average ± SEM of three assays, $p<0.001$ vs no preincubation by parametric Student's *t*-test for independent samples). Consistent with the above data, PGE_1 also inhibited rat lens AKR1B4 with an IC50 of 4.1 ± 1.12 μM. Finally, we assessed

Molecular Pharmacology Fast Forward. Published on October 20, 2015 as DOI: 10.1124/mol.115.100693
This article has not been copyedited and formatted. The final version may differ from this version.

the effect of PGA_1 on AKR1B4 activity in intact rat lenses by measuring the formation of sorbitol from glucose (Fig. 9). Incubation of intact lenses in a glucose enriched medium increased the formation of sorbitol. Interestingly, PGA_1 inhibited glucose-stimulated sorbitol formation in a concentration-dependent manner (Fig. 9A), showing a potency similar to that of other known inhibitors of AKRs like epalrestat (Fig. 9C). Moreover, PGE_1 was also an effective inhibitor in this system (Fig. 9B). Interestingly, PGE and PGE analogs are currently used for the treatment of various ocular pathologies, including glaucoma and ischemia (Alm, 2014; Steigerwalt et al., 2010). Since AKR inhibitors have been envisaged as potential therapeutic tools for ocular diabetic complications, the definition of PGs as inhibitors of AKR1B1 encourages the study of their potential usefulness for these conditions.

Molecular Pharmacology Fast Forward. Published on October 20, 2015 as DOI: 10.1124/mol.115.100693
This article has not been copyedited and formatted. The final version may differ from this version.

Discussion

Aldose reductase (AKR1B1) is an important drug target due to its involvement in many pathophysiological processes, including inflammation, allergy and the development of diabetic complications. Here we show that several PGs bind to and inhibit AKR1B1 by establishing specific interactions with the enzyme. Moreover, we have observed that PGA_1 and PGE_1 inhibit aldose reductase activity in an ex-vivo model of diabetic cataract. These observations, together with the fact that several PGs found to inhibit AKR1B1 are currently used in the clinical practice, open up new possibilities for designing novel therapeutic strategies to counteract the deleterious effects of aldose reductase in diabetic complications.

CyPGs modify a plethora of cellular proteins mainly at cysteine residues. However, their binding does not occur randomly; rather it is determined by structural features of the protein and the cyPG and by context factors. Aldose reductase was identified as a selective target for PGA_1 in murine fibroblasts, in which AKR enzymes appeared as the main cytosolic PGA_1-B-modified proteins (Díez-Dacal et al., 2011). Here we show that the major product of AKR1B1-PGA_1 interaction consists of a covalent adduct which incorporates one PG molecule. Thus, although AKR1B1 possesses seven cysteine residues, apparently only one is modified by PGA_1. Despite unsuccessful attempts to detect the modified peptide by MS analysis, our results are consistent with the hypothesis that PGA_1 interacts with Cys298, which occupies a key position in the active site of AKR1B1 (Balendiran et al., 2011). This is based on analogy with AKR1B10, which is modified at the equivalent Cys299, as detected by both MS (Díez-Dacal, unpublished results) and site directed mutagenesis (Díez-Dacal et al., 2011).

Cys298 of AKR1B1 has been shown to be the target for various oxidative modifications that are responsible for a complex regulation of AKR1B1 activity. Thus, some modifications, like S-nitrosylation or alkylation, may even increase the activity of the enzyme in vitro, whereas glutathionylation is inhibitory (Kaiserova et al., 2006; Srivastava et al., 2003). In vivo, sufenylation of the active site cysteines, Cys298 and Cys303, a modification potentially

Molecular Pharmacology Fast Forward. Published on October 20, 2015 as DOI: 10.1124/mol.115.100693
This article has not been copyedited and formatted. The final version may differ from this version.

secondary to S-nitrosylation, has been proposed to mediate the increase in AKR1B1 enzyme activity observed in the ischemic heart (Baba et al., 2009). Therefore, it seems that the functional consequences of the modification depend on the size or the structure of the modifying moiety. Covalent addition of cyPGs to cysteine residues requires the thiol group to be in its free thiolate form. Thus, other oxidative modifications of AKR1B1, including disulfide formation with the neighboring Cys303, will preclude covalent binding of PGA_1. Interestingly, although cyPG addition is considered irreversible under physiological conditions (Suzuki et al., 1997), our results demonstrate that the AKR1B1-PGA_1 adduct is not stable in the presence of millimolar GSH concentrations. Our molecular model shows that, although the binding of PGA_1 to the active site of AKR1B1 prevents the entry of GSH into the anion binding site (Singh et al., 2006), the GSH thiol group is accessible to C11 of PGA_1 and therefore, it could react with the cyPG and revert the covalent adduct (Fig. 3b), which is in accordance with our experimental results. These observations reinforce the importance of GSH levels as modulators of cyPG-induced protein modification and regulation, observed in several experimental models (Díez-Dacal et al., 2011; Gayarre et al., 2005; Straus et al., 2000). Moreover, they grant the study of the reversibility of other cyPG- or electrophilic lipid-protein adducts and the reevaluation of their potential regulatory importance.

An interesting aspect of PGA_1 is its high selectivity towards AKR1B1 versus AKR1A1, which is an important index for the adequacy of potential inhibitors. Inhibition of AKR1A1, also known as aldehyde reductase or ALR1, may result in skin reactions and liver toxicity (Muthenna et al., 2009). Therefore, lack of selectivity between the two enzymes is considered to be responsible for many of the adverse effects of compounds intended for inhibition of AKR1B1, which in some cases precludes their clinical use (El-Kabbani et al., 2004).

Importantly, we show that non-electrophilic PGs may also interact with AKR1B1 and act as inhibitors of the enzyme. Previous interactions of AKR1B1 with PGs have been reported. AKR1B1 has been identified as a PGF_2 synthase using PGH_2 as the substrate in the

presence of NADPH (Michaud et al., 2014), whereas in its absence it may catalyze its isomerization to PGD_2, which is a precursor for the J series of cyPGs (Nagata et al., 2011). In this context, our findings that several PGs bind and inhibit the enzyme may be highly relevant in pathophysiological settings. In the case of PGE_2 it is interesting to note that the enzyme-PG complex is stable enough as to be observed by MALDI-TOF MS under mild denaturing conditions, although is lost after removal of excess PG and under strong denaturing conditions, such as those used for SDS-PAGE or incubation in high guanidinium chloride concentrations. IC50 values obtained for most PGs were in the micromolar range. The differences found between IC50 values for recombinant AKR1B1 and the purified rat lens enzyme are likely due to differences in enzyme preparation and/or assay conditions.

The pathophysiological implications of AKR1B1 continue to expand. Besides its widely accepted role in the development of diabetic complications, AKR1B1 has been recently involved in tumorigenesis and in allergic responses (Yadav et al., 2013). The fact that AKR1B1 activity can be regulated by PGs poses interesting questions in this context. Remarkably, PGE_2 has been reported to exert protective effects in asthma, mainly through interaction with the PGE receptor (Torres et al., 2015), but an implication of AKR1B1 in these effects has not been explored. It would be relevant to assess whether AKR1B1 can be modulated by endogenously generated PGs and if so, if this influences inflammatory or allergic responses. Importantly, genetic alterations can provide additional pathophysiological implications of AKR1B1. Indeed, several polymorphisms of the AKR1B1 gene have been associated with the development of diabetic complications (Abhary et al., 2010; Demaine, 2003). Nevertheless, an association of these or other polymorphisms with tumorigenesis or inflammatory allergic conditions has not been reported to date. Studies are under way to explore these possibilities.

One of the most common diabetic complications is the development of diabetic cataracts. AKR1B1 has long been involved in lens opacification in situations of hyperglycaemia (Narayanan, 1993). AKR1B1 has been identified as a risk factor for cataract. Experimental aldose reductase overexpression in the lens accelerates the development of cataracts in

Molecular Pharmacology Fast Forward. Published on October 20, 2015 as DOI: 10.1124/mol.115.100693
This article has not been copyedited and formatted. The final version may differ from this version.

diabetic mice (Lee et al., 1995) (Snow et al., 2015), whereas knockdown of the enzyme in rats protects from lens opacification ex vivo (Reddy et al., 2011). In addition, strategies using inhibitors have provided numerous pieces of evidence for the implication of AKR1B1 in diabetic cataract in various experimental models. Thus, topical administration of an aldose reductase inhibitor delays the development of cataracts in diabetic dogs (Kador et al., 2010), whereas oral treatment with another inhibitor prevents their progression in rats (Kawakubo et al., 2012). The results herein presented show that both PGA_1 and PGE_1 reduce the formation of sorbitol in isolated rat lenses exposed to high glucose, thus opening the way for in vivo studies. Interestingly, the extent of inhibition attained by PGs is similar to that of the well-known AKR inhibitor epalrestat, which has a considerable lower IC50 value in vitro. Therefore, the possibility exists that a better penetrance or a more stable interaction with the enzyme favor the efficacy of PGs in this biological system. Interestingly, some of the PGs assayed, including PGE_1 (alprostadil) and its analog, limaprost, are currently used in the clinical practice as vasodilators, and beneficial effects of these agents have been documented in age-related macular degeneration (Augustin et al., 2013) and in intermittent claudication (Nakanishi et al., 2008), among others. In fact, several pharmaceutical presentations for topical ocular administration in the treatment of glaucoma are available, which include PG analogs at concentrations in the range of those used in this work. Therefore, our studies raise the possibilities of considering PGs as leading molecules for the design of new inhibitors and/or exploring the potential of the already clinically used PGs as therapeutic agents in the management of some diabetic complications.

In summary, the results presented here shed new light on the mechanism of action of cyPGs by showing that under certain conditions their binding to proteins may be reversible. Moreover, they unveil that various PGs, some of which are used in the clinic, are inhibitors of AKR1B1, thus suggesting an avenue for novel therapeutic opportunities.

Molecular Pharmacology Fast Forward. Published on October 20, 2015 as DOI: 10.1124/mol.115.100693
This article has not been copyedited and formatted. The final version may differ from this version.

Acknowledgements:

The technical assistance of MJ Carrasco is gratefully appreciated.

Author contributions:

Participated in research design: Pérez-Sala, Zimmerman, Sánchez-Gómez, Gago.

Conducted experiments: Díez-Dacal, Milackova, Sánchez-Gómez, Zimmerman, Ballekova, Sánchez-Murcia, Gharbi

Contributed reagents or analytic tools: Stefek, Gago, Sánchez-Murcia, Gharbi

Performed data analysis: Pérez-Sala, Sánchez-Gómez, Sánchez-Murcia, Díez-Dacal, Gharbi, Gago, Stefek

Wrote or contributed to the writing of the manuscript: Stefek, Gago, Agúndez, García-Martín, Pérez-Sala

References

Abhary S, Burdon KP, Laurie KJ, Thorpe S, Landers J, Goold L, Lake S, Petrovsky N and Craig JE (2010) Aldose reductase gene polymorphisms and diabetic retinopathy susceptibility. *Diabetes Care* **33**: 1834-1836.

Alexiou P, Pegklidou K, Chatzopoulou M, Nicolaou I and Demopoulos VJ (2009) Aldose reductase enzyme and its implication to major health problems of the 21(st) century. *Curr Med Chem* **16**(6): 734-752.

Alm A (2014) Latanoprost in the treatment of glaucoma. *Clin Ophthalmol* **8**: 1967-1985.

Augustin AJ, Diehm C, Grieger F and Bentz J (2013) Alprostadil infusion in patients with dry age related macular degeneration: a randomized controlled clinical trial. *Expert Opin Investig Drugs* **22**(7): 803-812.

Baba SP, Wetzelberger K, Hoetker JD and Bhatnagar A (2009) Posttranslational glutathiolation of aldose reductase (AKR1B1): a possible mechanism of protein recovery from S-nitrosylation. *Chem Biol Interact* **178**(1-3): 250-258.

Balendiran GK, Sawaya MR, Schwarz FP, Ponniah G, Cuckovich R, Verma M and Cascio D (2011) The role of Cys-298 in aldose reductase function. *J Biol Chem* **286**(8): 6336-6344.

Case DA, Berryman JT, Betz RM, Cerutti DS, T.E. Cheatham I, Darden TA, Duke RE, Giese TJ, Gohlke H, Goetz AW, Homeyer N, Izadi S, Janowski P, Kaus J, Kovalenko A, Lee TS, LeGrand S, Li P, Luchko T, Luo R, Madej B, Merz KM, Monard G, Needham P, Nguyen H, Nguyen HT, Omelyan I, Onufriev A, Roe DR, Roitberg A, Salomon-Ferrer R, Simmerling CL, Smith W, Swails J, Walker RC, Wang J, Wolf RM, Wu X, York DM and Kollman PA (2015) Amber 2015. *University of California, San Francisco*.

Cernuda-Morollón E, Pineda-Molina E, Cañada FJ and Pérez-Sala D (2001) 15-Deoxy-$\Delta^{12,14}$-prostaglandin J_2 inhibition of NF-κB DNA binding through covalent modification of the p50 subunit. *J Biol Chem* **276**: 35530-35536.

Chatzopoulou M, Mamadou E, Juskova M, Koukoulitsa C, Nicolaou I, Stefek M and Demopoulos VJ (2011) Structure-activity relations on [1-(3,5-difluoro-4-hydroxyphenyl)-1H-pyrrol-3-yl]phenylmethanone. The effect of methoxy substitution on aldose reductase inhibitory activity and selectivity. *Bioorg Med Chem* **19**(4): 1426-1433.

Demaine AG (2003) Polymorphisms of the aldose reductase gene and susceptibility to diabetic microvascular complications. *Curr Med Chem* **10**: 1389-1398.

Díez-Dacal B, Gayarre J, Gharbi S, Timms JF, Coderch C, Gago F and Pérez-Sala D (2011) Identification of aldo-keto reductase AKR1B10 as a selective target for modification and inhibition by PGA1: Implications for anti-tumoral activity. *Cancer Res* **71**: 4161-4171.

Díez-Dacal B and Pérez-Sala D (2012) A-class prostaglandins: early findings and new perspectives for overcoming tumor chemoresistance. *Cancer Lett* **320**: 150-157.

El-Kabbani O, Ruiz F, Darmanin C and Chung RP (2004) Aldose reductase structures: implications for mechanism and inhibition. *Cell Mol Life Sci* **61**(7-8): 750-762.

Fukushima S, Takeuchi Y, Kishimoto S, Yamashita S, Uetsuki K, Shirakawa S, Suzuki M, Furuta K, Noyori R, Sasaki H, Kikuchi Y, Kita T, Yamori T, Sawada J, Kojima M, Hazato A, Kurozumi S and Fukushima M (2001) Antitumor activity, optimum administration method and pharmacokinetics of 13,14-dihydro-15-deoxy-deoxy-Delta7 -prostaglandin A1 methyl ester (TEI-9826) integrated in lipid microspheres (Lipo TEI-9826). *Anticancer Drugs* **12**(3): 221-234.

Garzón B, Oeste CL, Díez-Dacal B and Pérez-Sala D (2011) Proteomic studies on protein modification by cyclopentenone prostaglandins: expanding our view on electrophile actions. *J Proteomics* **74**: 2243-2263.

Gayarre J, Stamatakis K, Renedo M and Pérez-Sala D (2005) Differential selectivity of protein modification by the cyclopentenone prostaglandins PGA_1 and 15-deoxy-$\Delta^{12,14}$-PGJ_2: role of glutathione. *FEBS Lett* **579**: 5803-5808.

Hanchanale V and Eardley I (2014) Alprostadil for the treatment of impotence. *Exp Opin Pharmacother* **15**(3): 421-428.

Hashim Z and Zarina S (2012) Osmotic stress induced oxidative damage: possible mechanism of cataract formation in diabetes. *J Diabetes Complications* **26**(4): 275-279.

Homem de Bittencourt PI, Jr., Lagranha DJ, Maslinkiewicz A, Senna SM, Tavares AM, Baldissera LP, Janner DR, Peralta JS, Bock PM, Gutierrez LL, Scola G, Heck TG, Krause MS, Cruz LA, Abdalla DS, Lagranha CJ, Lima T and Curi R (2007) LipoCardium: endothelium-directed cyclopentenone prostaglandin-based liposome formulation that completely reverses atherosclerotic lesions. *Atherosclerosis* **193**(2): 245-258.

Kabututu Z, Manin M, Pointud JC, Maruyama T, Nagata N, Lambert S, Lefrancois-Martinez AM, Martinez A and Urade Y (2009) Prostaglandin F2alpha synthase activities of aldo-keto reductase 1B1, 1B3 and 1B7. *J Biochem* **145**(2): 161-168.

Kador PF, Webb TR, Bras D, Ketring K and Wyman M (2010) Topical KINOSTAT ameliorates the clinical development and progression of cataracts in dogs with diabetes mellitus. *Vet Ophthalmol* **13**(6): 363-368.

Kaiserova K, Srivastava S, Hoetker JD, Awe SO, Tang XL, Cai J and Bhatnagar A (2006) Redox activation of aldose reductase in the ischemic heart. *J Biol Chem* **281**(22): 15110-15120.

Kawakubo K, Mori A, Sakamoto K, Nakahara T and Ishii K (2012) GP-1447, an inhibitor of aldose reductase, prevents the progression of diabetic cataract in rats. *Biol Pharm Bull* **35**(6): 866-872.

Kim EH and Surh YJ (2006) 15-deoxy-Delta12,14-prostaglandin J2 as a potential endogenous regulator of redox-sensitive transcription factors. *Biochem Pharmacol* **72**(11): 1516-1528.

Ko BC, Ruepp B, Bohren KM, Gabbay KH and Chung SS (1997) Identification and characterization of multiple osmotic response sequences in the human aldose reductase gene. *J Biol Chem* **272**(26): 16431-16437.

Laffin B and Petrash JM (2012) Expression of the Aldo-Ketoreductases AKR1B1 and AKR1B10 in Human Cancers. *Front Pharmacol* **3**: 104.

Lai KP, Law AY, Lau MC, Takei Y, Tse WK and Wong CK (2013) Osmotic stress transcription factor 1b (Ostf1b) promotes migration properties with the modulation of epithelial mesenchymal transition (EMT) phenotype in human embryonic kidney cell. *Int J Biochem Cell Biol* **45**(8): 1921-1926.

Lee AY, Chung SK and Chung SS (1995) Demonstration that polyol accumulation is responsible for diabetic cataract by the use of transgenic mice expressing the aldose reductase gene in the lens. *Proc Natl Acad Sci U S A* **92**(7): 2780-2784.

Levonen AL, Landar A, Ramachandran A, Ceaser EK, Dickinson DA, Zanoni G, Morrow JD and Darley-Usmar VM (2004) Cellular mechanisms of redox cell signaling: the role of cysteine modification in controlling antioxidant defenses in response to electrophilic lipid oxidation products. *Biochem J* **378**: 373-382.

Martínez AE, Sánchez-Gómez FJ, Díez-Dacal B, Oeste CL and Pérez-Sala D (2012) 15-deoxy-$\Delta^{12,14}$-prostaglandin J_2 exerts pro- and anti-inflammatory effects in mesangial cells in a concentration-dependent manner. *Inflamm Allergy Drug Targets* **11**: 58-65.

Michaud A, Lacroix-Pepin N, Pelletier M, Veilleux A, Noel S, Bouchard C, Marceau P, Fortier MA and Tchernof A (2014) Prostaglandin (PG) F2 alpha synthesis in human subcutaneous and omental adipose tissue: modulation by inflammatory cytokines and role of the human aldose reductase AKR1B1. *PLoS One* **9**(3): e90861.

Muthenna P, Suryanarayana P, Gunda SK, Petrash JM and Reddy GB (2009) Inhibition of aldose reductase by dietary antioxidant curcumin: mechanism of inhibition, specificity and significance. *FEBS Lett* **583**: 3637-3642.

Mylari BL, Armento SJ, Beebe DA, Conn EL, Coutcher JB, Dina MS, O'Gorman MT, Linhares MC, Martin WH, Oates PJ, Tess DA, Withbroe GJ and Zembrowski WJ (2003) A highly selective, non-hydantoin, non-carboxylic acid inhibitor of aldose reductase with potent oral activity in diabetic rat models: 6-(5-chloro-3-methylbenzofuran- 2-sulfonyl)-2-H-pyridazin-3-one. *J Med Chem* **46**: 2283-2286.

Nagata N, Kusakari Y, Fukunishi Y, Inoue T and Urade Y (2011) Catalytic mechanism of the primary human prostaglandin F2alpha synthase, aldo-keto reductase 1B1--

prostaglandin D2 synthase activity in the absence of NADP(H). *FEBS J* **278**: 1288-1298.

Nakanishi K, Tanaka M, Misawa H, Takigawa T and Ozaki T (2008) Midterm results of prostaglandin E1 treatment in patients with lumbar spinal canal stenosis accompanied by intermittent claudication. *Spine* **33**: 1465-1469.

Narayanan S (1993) Aldose reductase and its inhibition in the control of diabetic complications. *Ann Clin Lab Sci* **23**: 148-158.

Oeste CL and Pérez-Sala D (2014) Modification of cysteine residues by cyclopentenone prostaglandins: interplay with redox regulation of protein function. *Mass Spectrom Rev* **33**: 110-125.

Pérez-Sala D (2011) Electrophilic eicosanoids: signaling and targets. *Chem Biol Interact* **192**: 96-100.

Pollak N, Dolle C and Ziegler M (2007a) The power to reduce: pyridine nucleotides--small molecules with a multitude of functions. *Biochem J* **402**: 205-218.

Pollak N, Niere M and Ziegler M (2007b) NAD kinase levels control the NADPH concentration in human cells. *J Biol Chem* **282**: 33562-33571.

Ramana KV, Fadl AA, Tammali R, Reddy AB, Chopra AK and Srivastava SK (2006) Aldose reductase mediates the lipopolysaccharide-induced release of inflammatory mediators in RAW264.7 murine macrophages. *J Biol Chem* **281**: 33019-33029.

Reddy AB, Tammali R, Mishra R, Srivastava S, Srivastava SK and Ramana KV (2011) Aldose reductase deficiency protects sugar-induced lens opacification in rats. *Chem Biol Interact* **191**: 346-350.

Sánchez-Gómez FJ, Díez-Dacal B, Pajares MA, Llorca O and Pérez-Sala D (2010) Cyclopentenone prostaglandins with dienone structure promote cross-linking of the chemoresistance-inducing enzyme Glutathione Transferase P1-1. *Mol Pharmacol* **78**: 723-733.

Snow A, Shieh B, Chang KC, Pal A, Lenhart P, Ammar D, Ruzycki P, Palla S, Reddy GB and Petrash JM (2015) Aldose reductase expression as a risk factor for cataract. *Chem Biol Interact*. **234:** 247-253.

Srivastava SK, Ramana KV, Chandra D, Srivastava S and Bhatnagar A (2003) Regulation of aldose reductase and the polyol pathway activity by nitric oxide. *Chem Biol Interact* **143-144**: 333-340.

Srivastava SK, Yadav UC, Reddy AB, Saxena A, Tammali R, Shoeb M, Ansari NH, Bhatnagar A, Petrash MJ, Srivastava S and Ramana KV (2011) Aldose reductase inhibition suppresses oxidative stress-induced inflammatory disorders. *Chem Biol Interact* **191**: 330-338.

Steigerwalt RD, Jr., Cesarone MR, Belcaro G, Pascarella A, De Angelis M, Gattegna R and Nebbioso M (2010) Arteritic anterior ischemic optic neuropathy treated with intravenous prostaglandin E(1) and steroids. *Int J Angiol* **19**: e113-115.

Straus DS, Pascual G, Li M, Welch JS, Ricote M, Hsiang CH, Sengchanthalangsy LL, Ghosh G and Glass CK (2000) 15-deoxy-delta 12,14-prostaglandin J2 inhibits multiple steps in the NF- kappa B signaling pathway. *Proc Natl Acad Sci U S A* **97**: 4844-4849.

Suzen S and Buyukbingol E (2003) Recent studies of aldose reductase enzyme inhibition for diabetic complications. *Curr Med Chem* **10**: 1329-1352.

Suzuki M, Mori M, Niwa T, Hirata R, Furuta K, Ishikawa T and Noyori R (1997) Chemical implications for antitumor and antiviral prostaglandins: reaction of D^7-prostaglandin A_1 and prostaglandin A_1 methyl esters with thiols. *J Am Chem Soc* **119**: 2376-2385.

Swainston Harrison T and Plosker GL (2007) Limaprost. *Drugs* **67**: 109-118; discussion 119-120.

Talosi G, Katona M, Racz K, Kertesz E, Onozo B and Turi S (2004) Prostaglandin E1 treatment in patent ductus arteriosus dependent congenital heart defects. *J Perinatal Med* **32**: 368-374.

Tang WH, Stitham J, Gleim S, Di Febbo C, Porreca E, Fava C, Tacconelli S, Capone M, Evangelista V, Levantesi G, Wen L, Martin K, Minuz P, Rade J, Patrignani P and Hwa J (2011) Glucose and collagen regulate human platelet activity through aldose reductase induction of thromboxane. *J Clin Invest* **121**: 4462-4476.

Torres R, Picado C and de Mora F (2015) The PGE2-EP2-mast cell axis: an antiasthma mechanism. *Mol Immunol* **63**: 61-68.

van Iersel ML, Cnubben NH, Smink N, Koeman JH and van Bladeren PJ (1999) Interactions of prostaglandin A2 with the glutathione-mediated biotransformation system. *Biochem Pharmacol* **57**: 1383-1390.

Vedantham S, Thiagarajan D, Ananthakrishnan R, Wang L, Rosario R, Zou YS, Goldberg I, Yan SF, Schmidt AM and Ramasamy R (2014) Aldose reductase drives hyperacetylation of Egr-1 in hyperglycemia and consequent upregulation of proinflammatory and prothrombotic signals. *Diabetes* **63**: 761-774.

Yadav UC, Mishra R, Aguilera-Aguirre L, Sur S, Bolodgh I, Ramana KV and Srivatsava SK (2013) Prevention of allergic rhinitis by aldose reductase inhibition in a murine model. *Inflamm Allergy Drug Targets* **12**: 178-186.

Yadav UC, Ramana KV and Srivastava SK (2011) Aldose reductase inhibition suppresses airway inflammation. *Chem Biol Interact* **191**: 339-345.

Ying W (2008) NAD+/NADH and NADP+/NADPH in cellular functions and cell death: regulation and biological consequences. *Antioxid Redox Signal* **10**: 179-206.

Zhang P, Xing K, Randazzo J, Blessing K, Lou MF and Kador PF (2012) Osmotic stress, not aldose reductase activity, directly induces growth factors and MAPK signaling changes during sugar cataract formation. *Exp Eye Res* **101**: 36-43.

Footnotes

Beatriz Díez-Dacal and Francisco J. Sánchez-Gómez contributed equally to this work.

This work has been funded by grants from the Spanish Ministerio de Economía y Competitividad [SAF2009-11642] (Supported in part by FEDER) and [SAF2012-36519] and Instituto de Salud Carlos III (RETIC RIRAAF) [RD12/0013/0008] to DPS; Instituto de Salud Carlos III (RETIC RIRAAF) [RD12/0013/0002] to JAGA; Slovak Grant Agency [VEGA 2/0041/15] to MS; the Spanish Ministerio de Economía y Competitividad [SAF2012-39760-C02-02] and Comunidad Autómoma de Madrid [S2010-BMD-2457] to FG. The collaboration and Short Term Scientific Missions between DPS and MS laboratories have been supported by COST Action CM1001.

Please address reprints requests to:

Dr. Dolores Pérez-Sala

Department of Chemical and Physical Biology

Centro de Investigaciones Biológicas, C.S.I.C.

Ramiro de Maeztu, 9, 28040 Madrid, Spain

Phone: 34918373112

FAX: 34915360432

Email: dperezsala@cib.csic.es

Molecular Pharmacology Fast Forward. Published on October 20, 2015 as DOI: 10.1124/mol.115.100693
This article has not been copyedited and formatted. The final version may differ from this version.

Figure legends

Fig. 1. Effect of PGA_1 on AKR1B1 activity. (A) The activity of recombinant AKR1B1 was assayed in the presence of the indicated concentrations of PGA_1. The inset shows a sigmoidal plot for the calculation of IC50. (B) AKR1B1 was preincubated with 20 μM PGA_1 for the indicated times at r.t., after which, the incubation mixture was diluted ten times in the assay mixture and AKR1B1 activity was measured as detailed in Methods. (C) AKR1B1 was preincubated for 2 h at r.t. with the indicated concentrations of PGA_1. Incubation mixtures were then assayed for AKR1B1 activity in the presence of either the same concentrations of PGA_1 in the assay mixture (○) or after diluting the incubation mixture 10-times (●). In all cases, results are average values of three experiments performed in duplicate ± S.E.M.

Fig. 2. Interaction of PGA_1 with AKR1B1. (A) AKR1B1 at 5 μM was incubated with 50 μM PGA_1 for 1 h at r.t. Incubation mixtures were analyzed by MALDI-TOF MS, before (upper panel, -ZipTip) of after denaturation with guanidinium chloride and purification on ZipTip (lower panel). (B) AKR1B1 was incubated with PGA_1-B as above and the incorporation of the PG was assessed by SDS-PAGE, blot and detection of the biotin signal with HRP-streptavidin. The amount of protein was assessed by western blot with an anti-AKR antibody. Results are representative from at least three assays with similar results in each case.

Fig. 3. Covalent binding of PGA_1 to the catalytic Cys298 of AKR1B1. (A) Proposed mechanism of PGA_1 binding. (B) Molecular model of the binding of GSH to the active site of AKR1B1 (PDB entry: 1ADS) once PGA_1 is covalently bonded to Cys298. Dotted line indicates the proximity of thiol group in GSH to C11 of PGA_1.

Fig. 4. Effect of GSH on the stability of the AKR1B1- and AKR1B10-PGA_1-B adducts. AKR1B1 (A and B) or AKR1B10 (C) was incubated in the presence of 1 μM PGA_1-B, for 2 h at 37ºC. Where indicated, GSH or NBG at 5 mM final concentration was then added and the incubation was continued for 5 min at r.t. Samples were immediately processed for

SDS-PAGE by addition of Laemmli buffer and incubation at 95ºC for 5 min. Levels of the corresponding AKR-PGA_1-B adducts were assessed by SDS-PAGE, blot and biotin detection with HRP-streptavidin. Levels of AKR1B1 or AKR1B10 were assessed by western blot with an anti-AKR antibody. Lower panels show the quantitation of the biotin signals corrected by the levels of AKR protein. Results shown are average values of three determinations ± S.E.M. *p<0.05 vs control incubation. Dotted lines indicate where lanes from the same gel have been cropped.

Fig. 5. Involvement of cys298 in the interaction of PGA_1 with AKR1B1. (A) Interaction of PGA_1 with an AKR1B1 synthetic peptide. The synthetic peptide ^{297}VCALLSCTSHK^{307} was incubated with vehicle or PGA_1 and the peaks corresponding to the unmodified peptide (*m/z* 1161.5, upper panel) and the PGA_1-peptide adduct (*m/z* 1498.1, lower panel) were fragmented by MALDI-TOF-TOF MS-MS and the sequences obtained are shown. Asterisks and pound symbols denote the ions for which peaks compatible with the addition of PGA_1 on Cys303 and Cys298, respectively, were observed. (B) AKR1B1 was incubated with or without 100 μM GSNO for 30 min at r.t. The reaction mixtures were then incubated with 1 μM PGA_1-B for 90 min at r.t. AKR1B1 modification was analyzed by SDS-PAGE and blot with HRP-Streptavidin and protein levels assessed with an anti-AKR antibody. Lower panel depicts the quantitation of biotin signal corrected by AKR1B1 levels. Results shown are average values of three determinations ± S.E.M. *p<0.05 vs the absence of GSNO.

Fig. 6. Inhibition of AKR1B1 by various compounds. (A) Structure of some of the PGs and PG analogs studied as inhibitors of AKR1B1. (B) The activity of AKR1B1 in the presence of increasing concentrations of various compounds was assessed as in Figure 1A and the IC50 values obtained are shown. Assays were performed without preincubation except in the case of PGA_1-B for which a 2 h preincubation and subsequent 1:10 dilution in the assay mixture were performed. Results are average values ± S.E.M. of at least three determinations.

Fig. 7. PGE_2 interacts non-covalently with AKR1B1. (A) AKR1B1 at 5 μM was incubated with 50 μM PGE_2 for 1 h at r.t. Incubation mixtures were analyzed by MALDI-TOF MS,

Molecular Pharmacology Fast Forward. Published on October 20, 2015 as DOI: 10.1124/mol.115.100693
This article has not been copyedited and formatted. The final version may differ from this version.

before (upper panel, -ZipTip) or after denaturation with guanidinium chloride and purification on ZipTip (lower panel). (B) AKR1B1 was incubated with biotinylated PGA_1 (PGA_1-B or biotinylated PGE_2 (PGE_2-B) at the indicated concentrations for 2 h at r.t. and the incorporation of biotin was assessed by SDS-PAGE, transfer and detection with HRP-streptavidin. Levels of AKR1B1 were detected by western blot with anti-AKR antibody. Results are representative of three assays with the same results. (C) AKR1B1 was incubated with the indicated PGs at 100 μM, final concentration, during 30 min at r.t. Incubation mixtures were split into two aliquots and one of them was subjected to gel filtration on Zeba desalting micro-spin columns to remove excess PG (left panels). Subsequently, 1 μM PGA_1-B was added and incubation was continued for 90 min at r.t. before analysis by SDS-PAGE, blot and biotin detection with HRP-streptavidin or AKR1B1 detection with an anti-AKR antibody. Results shown are representative of three experiments with similar results. Dotted lines indicate where lanes from the same gel have been cropped.

Fig. 8. Effect of PGA_1 on AKR1A1 activity. Recombinant AKR1A1 was incubated in the presence of the indicated concentrations of PGA_1 and enzymatic activity was determined as described in the experimental section. Results are average values + SEM from 4 independent incubations. No statistically significant differences were found.

Fig. 9. PGA_1 inhibits aldose reductase activity in isolated rat lens. Isolated rat lenses were incubated with 50 mM glucose in the absence or presence of the indicated concentrations of PGA_1 (A), PGE_1 (B) or Epalrestat (C) for 3 h at 37ºC. The formation of sorbitol was monitored as described in Methods. Results are mean values + SEM from at least 4 independent incubations. +++ $p<0,001$ vs. Control; * $p<0,05$ and *** $p<0,001$ vs. 0 PGA_1. The control value in the absence of glucose represents the native sorbitol level in non-incubated lenses of control animals.

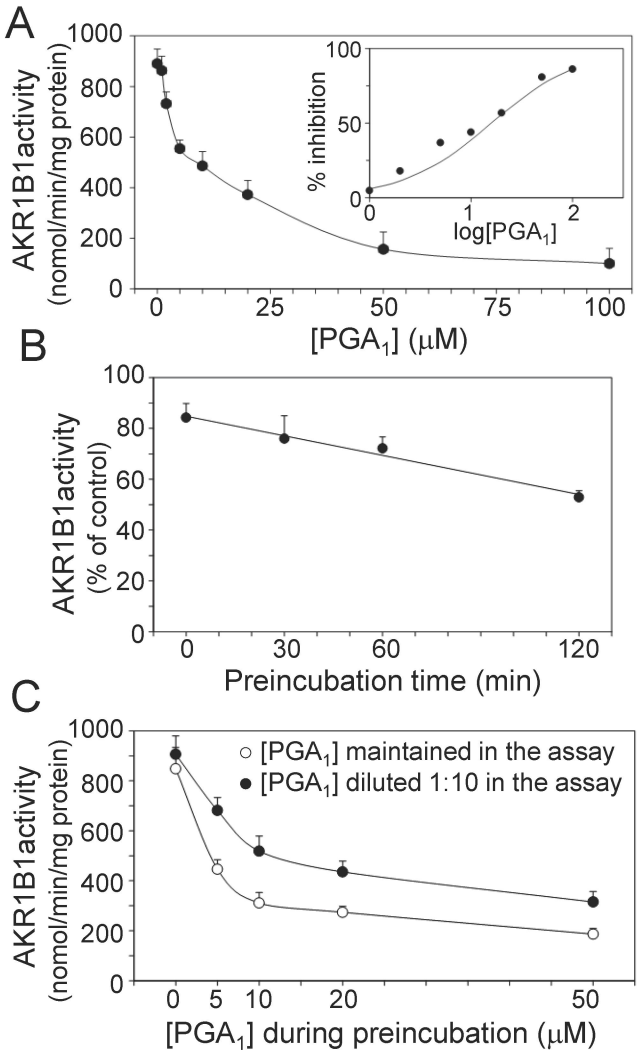
A
AKR1B1activity
(nomol/min/mg protein)
1000
800
600
400
200
0
0
25
50
75
100
[PGA1] (μM)
% inhibition
100
50
0
0
1
2
log[PGA1]
B
AKR1B1activity
(% of control)
100
80
60
40
20
0
0
30
60
120
Preincubation time (min)
C
AKR1B1activity
(nomol/min/mg protein)
1000
800
600
400
200
0
[PGA1] maintained in the assay
[PGA1] diluted 1:10 in the assay
0
5
10
20
50
[PGA1] during preincubation (μM)

Fig. 1

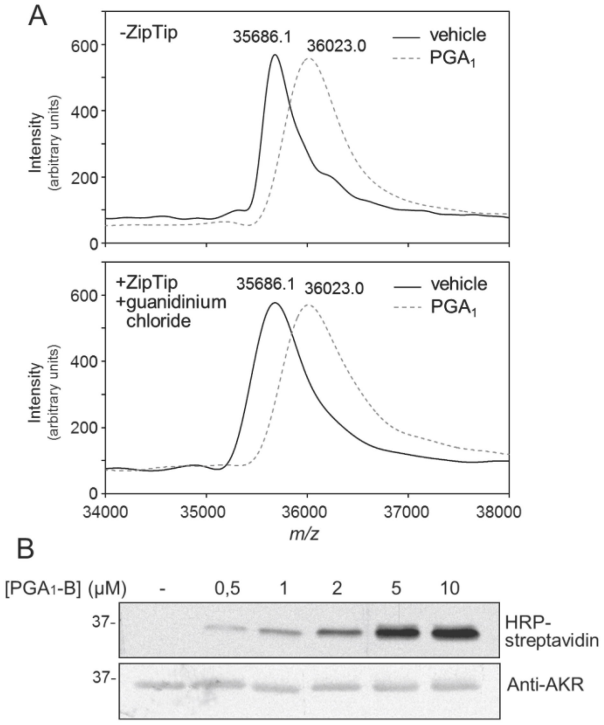
A
-ZipTip
35686.1
36023.0
vehicle
PGA1
Intensity
(arbitrary units)
600
400
200
0
+ZipTip
+guanidinium
chloride
35686.1
36023.0
vehicle
PGA1
Intensity
(arbitrary units)
600
400
200
0
34000
35000
36000
37000
38000
m/z
B
[PGA1-B] (μM)
-
0,5
1
2
5
10
37-
HRP-
streptavidin
37-
Anti-AKR

Fig. 2

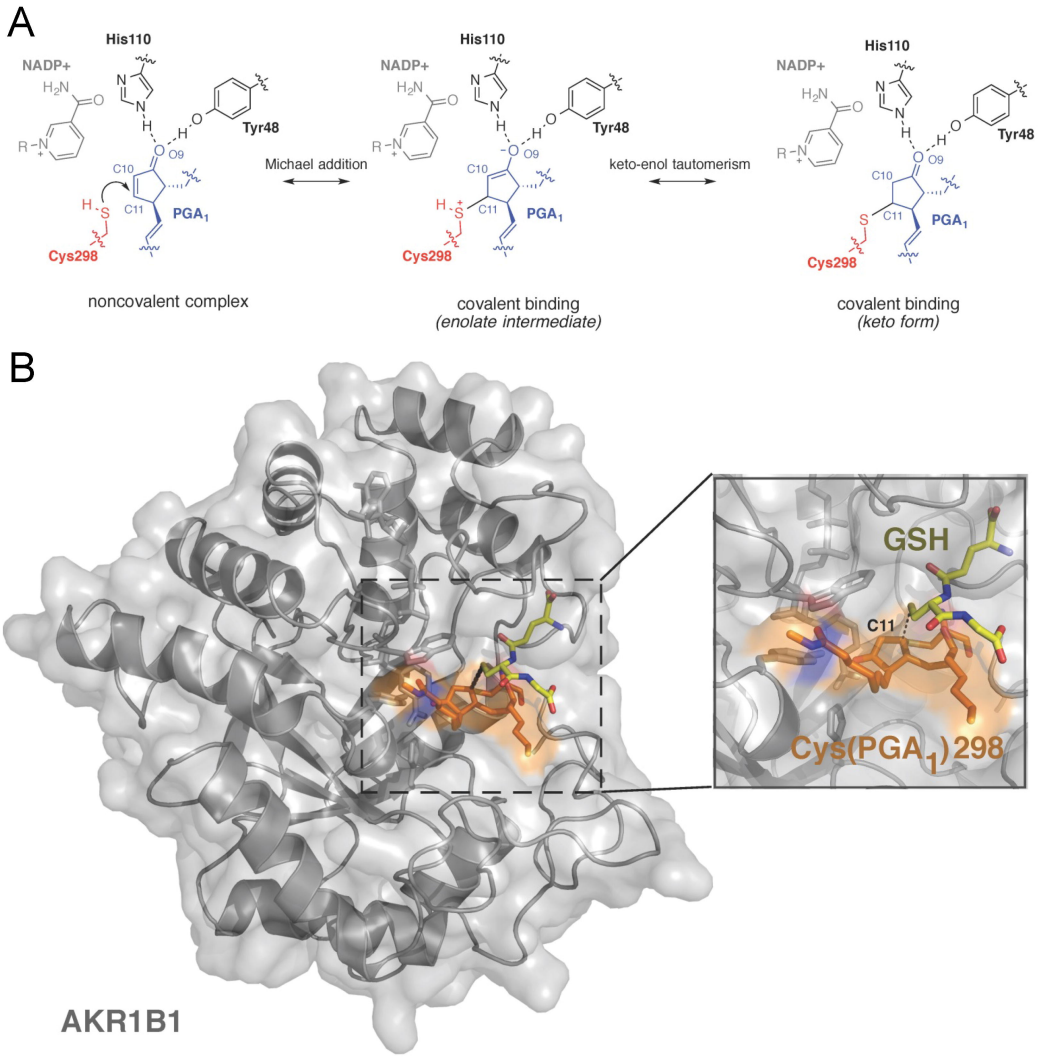
A
His110
NADP+
Tyr48
Cys298
PGA1
C10
C11
O9
Michael addition
keto-enol tautomerism
noncovalent complex
covalent binding
(enolate intermediate)
covalent binding
(keto form)
B
AKR1B1
GSH
C11
Cys(PGA1)298

Fig. 3

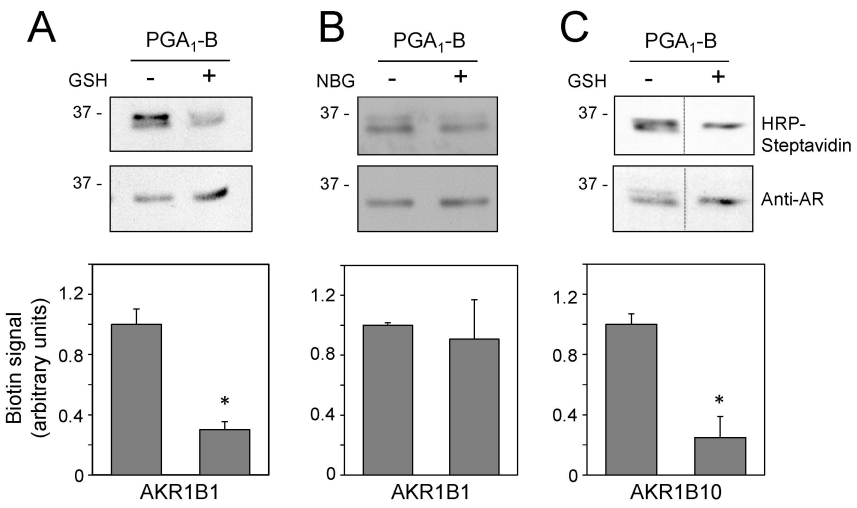
A
PGA1-B
GSH
-
+
37 -
37 -
B
PGA1-B
NBG
-
+
37 -
37 -
C
PGA1-B
GSH
-
+
37 -
37 -
HRP-
Steptavidin
Anti-AR
Biotin signal
(arbitrary units)
1.2
0.8
0.4
0
*
AKR1B1
AKR1B1
AKR1B10

Fig. 4

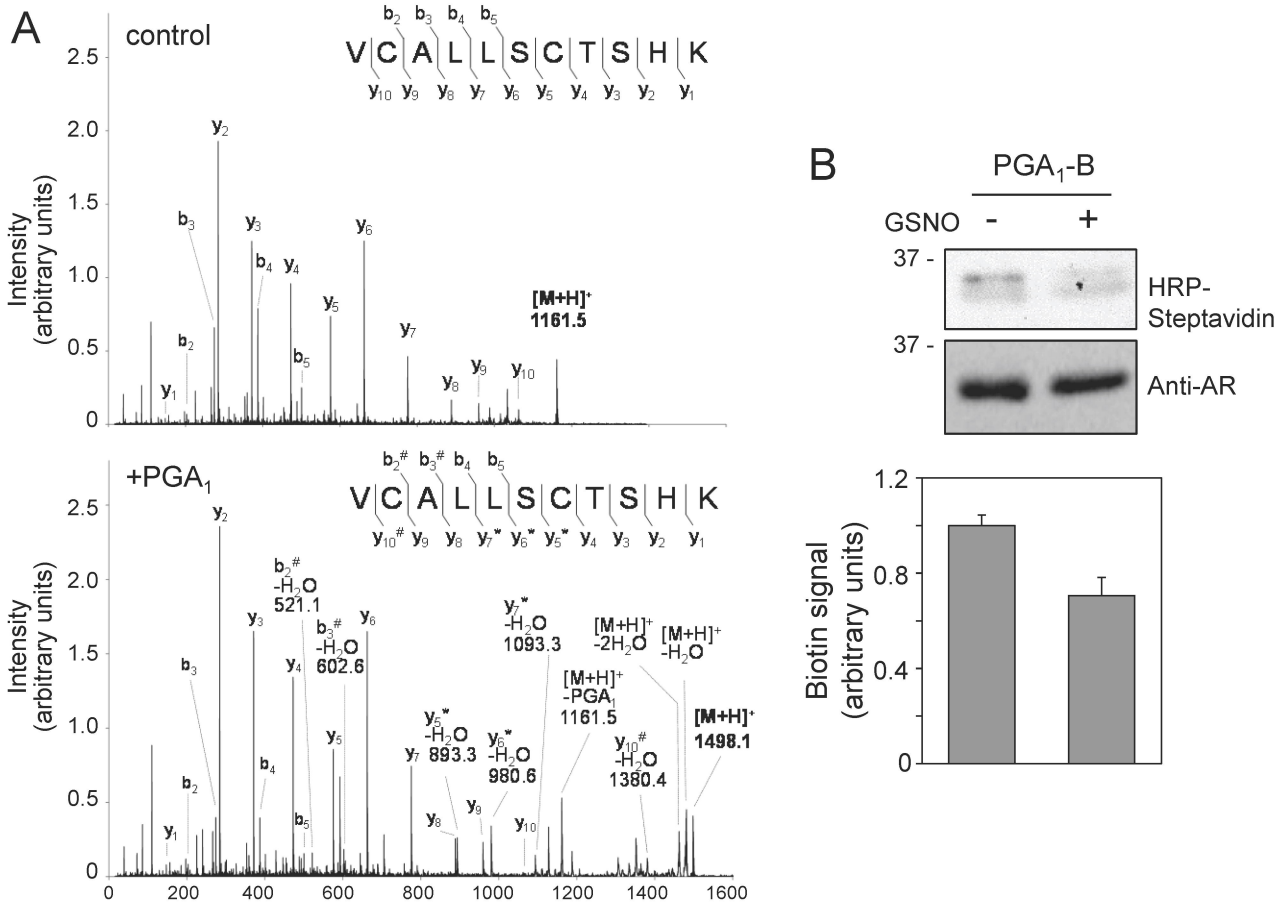
A
control
V C A L L S C T S H K
Intensity (arbitrary units)
[M+H]+ 1161.5
+PGA1
[M+H]+ -PGA1 1161.5
[M+H]+ 1498.1
B
PGA1-B
GSNO - +
37 -
HRP-Steptavidin
Anti-AR
Biotin signal (arbitrary units)

Fig. 5

A

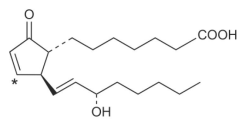

PGA_1

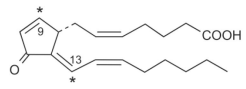

$15d\text{-}PGJ_2$

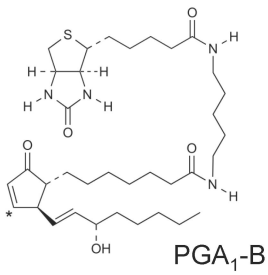

PGA_1-B

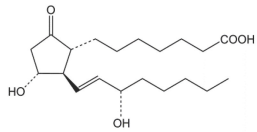

PGE_1

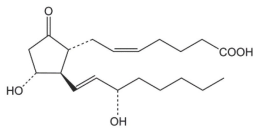

PGE_2

B

Compound	IC50 (μM)
PGA_1	15.9 ± 7.4
$15d\text{-}PGJ_2$	17.0 ± 4.4
$9,10\text{-dihydro-}15d\text{-}PGJ_2$	27.3 ± 5.2
PGE_2	49.4 ± 12.0
PGE_1	42.7 ± 10.6
Limaprost	123.3 ± 44.3
PGA_1-B	78.9 ± 16.5
AD-5467	0.4 ± 0.2

Fig. 6

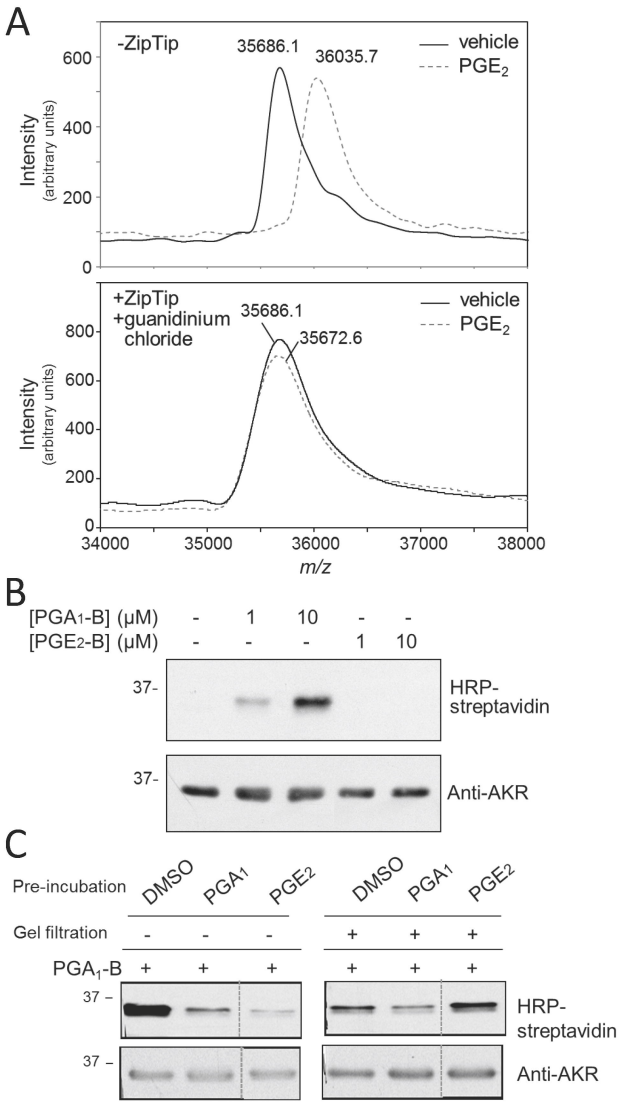
A
-ZipTip
35686.1
36035.7
vehicle
PGE2
Intensity (arbitrary units)
600
400
200
0
+ZipTip
+guanidinium chloride
35686.1
35672.6
vehicle
PGE2
Intensity (arbitrary units)
800
600
400
200
0
34000
35000
36000
37000
38000
m/z
B
[PGA1-B] (μM) - 1 10 - -
[PGE2-B] (μM) - - - 1 10
37-
HRP-streptavidin
37-
Anti-AKR
C
Pre-incubation
DMSO
PGA1
PGE2
DMSO
PGA1
PGE2
Gel filtration
- - - + + +
PGA1-B + + + + + +
37 –
HRP-streptavidin
37 –
Anti-AKR

Fig. 7

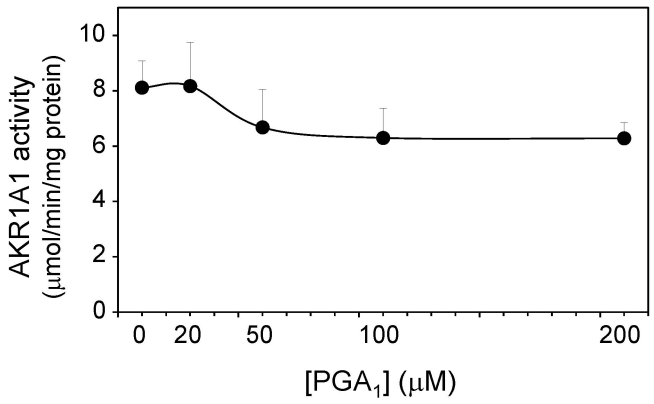
AKR1A1 activity
(μmol/min/mg protein)
10
8
6
4
2
0
0
20
50
100
200
[PGA1] (μM)

Fig. 8

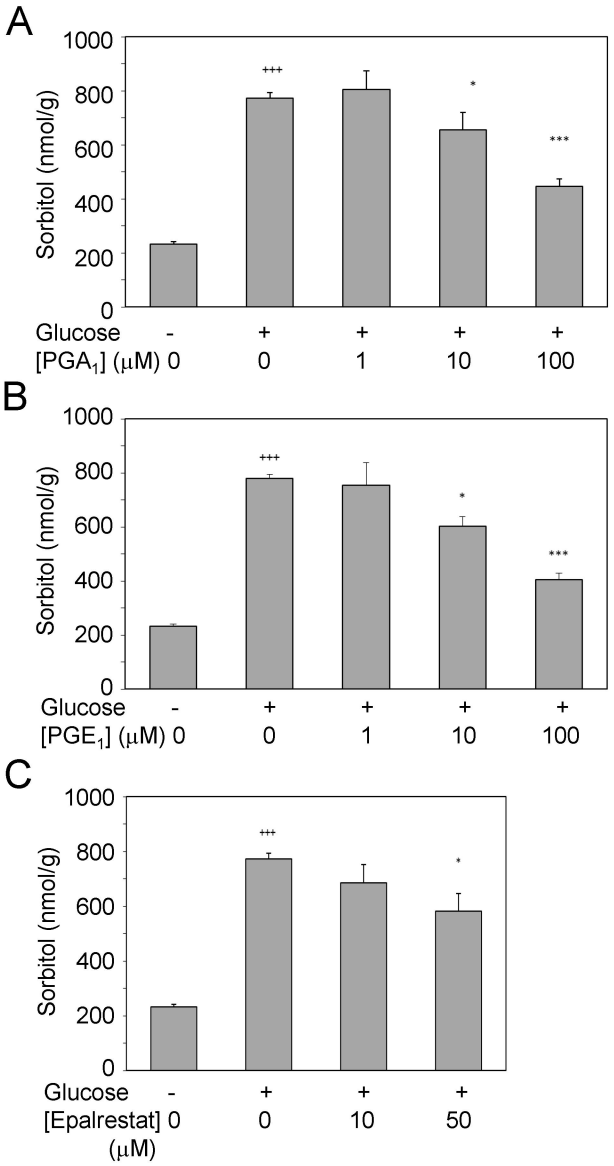
A
1000
800
600
400
200
0
Sorbitol (nmol/g)
+++
*
***
Glucose - + + + +
[PGA1] (μM) 0 0 1 10 100
B
1000
800
600
400
200
0
Sorbitol (nmol/g)
+++
*
***
Glucose - + + + +
[PGE1] (μM) 0 0 1 10 100
C
1000
800
600
400
200
0
Sorbitol (nmol/g)
+++
*
Glucose - + + +
[Epalrestat] 0 0 10 50
(μM)

Fig. 8